High-Performance Organic Field-Effect Transistors with Directionally Aligned Conjugated Polymer Film Deposited from Pre-Aggregated Solution

Nam-Koo Kim,[†] Soo-Young Jang,[†] Giuseppina Pace,[‖] Mario Caironi,[‖] Won-Tae Park[§], Dongyoon Khim[§], Juhwan Kim,[#] Dong-Yu Kim*[†], and Yong-Young Noh*[§]

[†]Department of Nanobio Materials and Electronics, School of Material Science and Engineering, Heeger Center for Advanced Materials, Gwangju Institute of Science and Technology (GIST), 261 Cheomdan-gwagiro (Oryong-dong), Buk-gu, Gwangju 500-712, Republic of Korea

[§]Department of Energy and Materials Engineering, Dongguk University, 26 Pil-dong, 3-ga, Jung-gu, Seoul 100-715, Republic of Korea,

[‖]Center for Nano Science and Technology @PoliMi, Istituto Italiano di Tecnologia, Via Pascoli 70/3, 20133 Milano, Italy,

[#]Department of Chemical Engineering and Material Science, University of California, Irvine, California 92697, United States

ABSTRACT: In this report, we investigate a formation mechanism for polymer chains aligned with various semiconductor polymers, and a microstructure for directionally aligned film through systematic analysis that includes polarized UV-visible-Near Infrared (UV-vis-NIR) absorption spectroscopy, atomic force microscope, polarized charge modulation microscopy (*p*-CMM), and incident X-ray diffraction (GIXD) measurements. Through this study, we make two important observations: first, the highly aligned organic polymer semiconductor films are achieved by off-center spin coating of the pre-aggregated conjugated polymer solution. Second, the directionally aligned conjugated polymer films exhibit a larger anisotropy on the top surface compared with bulk film, which allows effective mobility improvement in top-gate/bottom-contact field-effect transistors with high performance uniformity. Finally, we demonstrate high-mobility organic field-effect transistors (OFETs) (7.25 cm^2/Vs) with a mobility large anisotropy (37-fold) using poly[(E)-1,2-(3,3′-dioctadecyl-2,2′- dithienyl)ethylene-alt-dithieno-(3,2-b:2′,3′-d)thiophene] (P18) as the semiconductor layer.

INTRODUCTION

Solution-processed organic semiconductors (OSCs) represent valuable alternatives to the most traditional technologies employed thus far for conventional inorganic transistor fabrication through cost-effective and large-area printing processing. Organic field-effect transistors (OFETs) have significant potential to be implemented in flexible devices, paving the way for wearable electronic applications. The use of flexible substrates and low thermal treatments also allows the exploration of new applications currently not accessible with conventional inorganic transistors.[1-3] Recently, the field-effect mobility (μ_{FET}) measured in solution-processed OFETs has been shown to reach 10 cm^2/Vs, thus strongly extending the applicability of OFET technology.[4-8] The μ_{FET} in OFETs is strongly affected by the chemical composition of the semiconducting polymer,[9] as well as by its purity and molecular weight distribution,[10] which demand further effort during the synthesis process. The choice of deposition technique can also strongly affect semiconductor morphology, leading to the formation of films with different degrees of long-range structural order and chain packing. Moreover, charge transport in OFETs occurs in a limited volume at the semiconductor-dielectric interface, where interfacial defects and/or dipolar disorders can induce a distribution of trap states.[11,12] Various strategies have been followed to improve OFET performance, such as synthesizing advanced chemical structures, controlling molecular weight and purity, and optimizing the annealing process, semiconductor-dielectric, and electrode-semiconductor interfaces, as well as the device geometry.[13-20]

High μ_{FET} in OFETs has recently been achieved with state-of-the-art, electron-donor-acceptor (D-A) copolymers by improving the coplanarity along the D-A chain by chemical design, thus leading to effective control over the polymer chain alignment in the solid film. This is particularly effective if the polymer has liquid-crystal-like behavior.[21,22] Among the most successful strategies employed to align polymer chains, we can cite the slow drying of

the polymer semiconductors into nano-grooved substrates,[6,23] template-assisted self-assembly using a polydimethylsiloxane (PDMS) mold,[24,25] and off-center spin-coating, where the centripetal and centrifugal forces provided by the substrate spinning process are translated into fluid dynamic aligning forces.[7,10,26] In particular, the degree of pre-aggregation in the solution prior to deposition is often found to be the key for the formation of highly aligned domains in the polymer film.[10,27-30] The aggregates usually grow anisotropically along the alkyl stacking and conjugated backbone direction,[31] and pre-aggregated polymer OFETs showed significantly improved and largely anisotropic μ_{FET} from those with a well-dissolved solution.[27,32-34] Therefore, the strategy of adopting polymer solutions characterized by a high degree of pre-aggregation in the solution certainly has a strong potential for enhancing charge carrier properties with high uniformity over large areas when the polymers are effectively aligned in the channel of an OFET.

In this work, we investigate the effectiveness of polymer chain alignment induced by the fluid dynamic forces originated by the off-center spinning process. We selected the off-center spin-coating method because of its simple processing performed with a conventional spin-coater. In particular, we describe the influence of such processing on the μ_{FET} improvement of different semiconducting polymers. A combination of various techniques has been chosen to characterize both the bulk film properties through polarized UV-vis-NIR absorption spectroscopy and grazing incident X-ray diffraction (GIXD) measurements, as well as to characterize surface properties by atomic force microscopy (AFM) and polarized charge modulation microscopy (*p*-CMM).[35]

RESULTS AND DISCUSSION

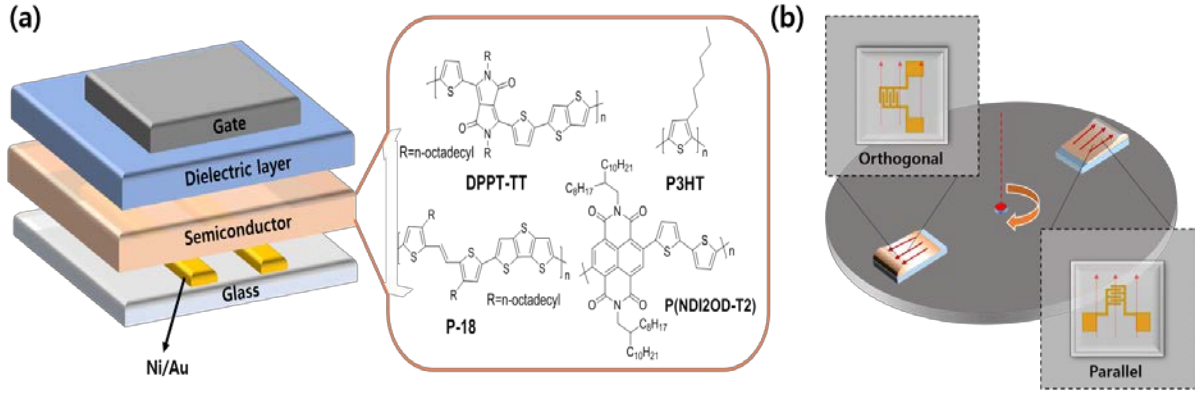

Figure 1. (a) TG/BC OFET device architecture with molecular structures for DPPT-TT, P-18, P3HT, and P(NDI2OD-T2); (b) Schematic illustration for off-center coating method with orthogonal and parallel coated directions from source to drain channels.

In the off-center spin coating, the interdigitated electrode pattern is located far from the spin center. The centripetal and centrifugal forces induced by the fast rotation of the spin-coater can drive the polymer chains to align along the radial direction. We define two main orientations for the samples: parallel, where the radial forces are parallel to the transistor channel, and orthogonal, where the radial forces are orthogonal to the channel (Figure 1b). In the commonly adopted on-center spin-coating, the sample is instead centered on the spin-coater, thus subjecting the electrode pattern to much more limited centrifugal and centripetal forces, with the inertial forces not substantially contributing to the alignment of polymer chains.

We observed that the best alignment of the polymer semiconductor films was achieved by off-center spin-coating from those solutions where polymer chain pre-aggregation was present. The chain alignment is found not to be a bulk property, but it is rather mostly localized at the polymer film surface. We also correlated the high degree of alignment to the strong μ_{FET} anisotropy (approximately 37 times in μ_{FET}) in the high-mobility polymer poly[(E)-1,2-(3,3′-dioctadecyl-2,2′-dithienyl)ethylene-alt-dithieno-(3,2-b:2′,3′-d)thiophene] (P18) as the semiconductor layer, thus achieving a maximum mobility of ~7.25 cm^2/Vs.[36] To generalize our

findings, we also compared our data with OFETs fabricated using widely known semiconductor polymers, such as diketopyrrolopyrrole thieno[3,2-b]thiophene (DPPT-TT), poly(3-hexylthiophene) (P3HT), and poly{[N,N′-bis(2-octyldodecyl)-1,4,5,8-naphthalenediimide-2,6-diyl]-alt-5,5′-(2,2′-bithiophene)} (P(NDI2OD-T2)).

The adopted device structure is a top-gate/bottom-contact (TG/BC) FET, where we used poly(methylmethacrylate) (PMMA) or CYTOP as the dielectric layer (Figure 1a). For the off-center spin-coating, the device pattern was located at approximately 2 cm from the axis center, subjecting the entire substrate to centrifugal forces that lead to the alignment of polymer chains (Figure 1b).

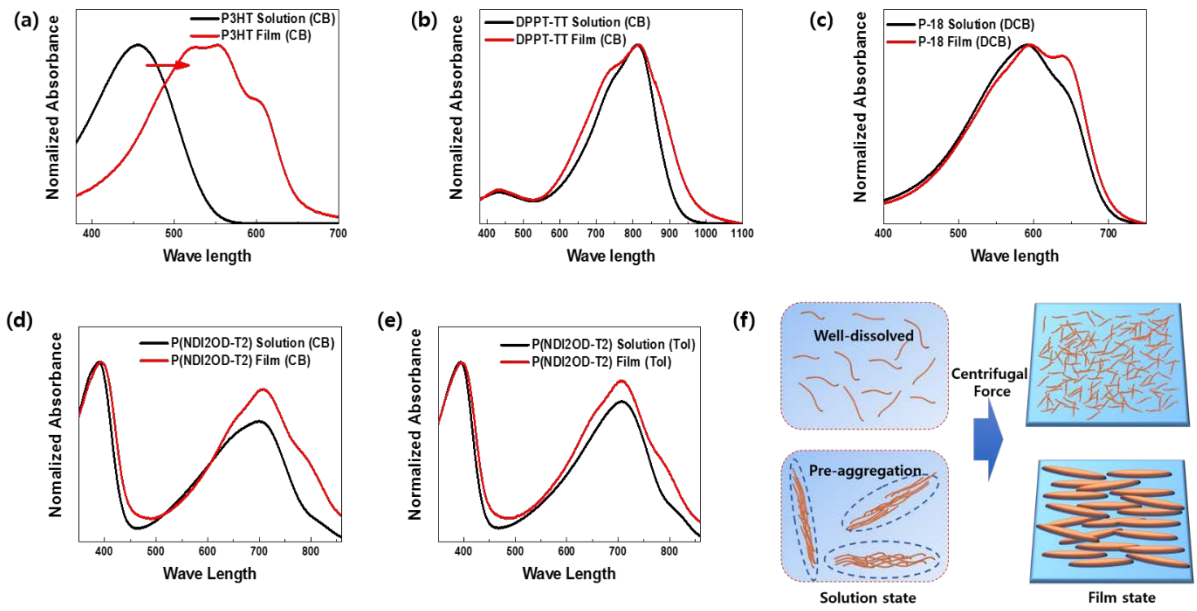

Figure 2. UV-vis-NIR absorption spectra of conjugated polymer solutions and films: (a) P3HT, (b) DPPT-TT, (c) P-18, (d) P(NDI2OD-T2) (chlorobenzene, CB), (e) P(NDI2OD-T2) (toluene, Tol), and (f) schematic illustration of well-dissolved and pre-aggregated polymer in solution and solid-state.

Figure 2 shows the UV-vis-NIR absorption spectra of the different polymers under study both in the solution and solid state, i.e., spin-coated thin films. The UV-vis-NIR absorption spectra of the P3HT film showed a significant red shift (approximately 100 nm) in the absorption maximum (λ_{max}) with respect to the solution spectra, indicating a strong chain

rearrangement in the solid state. On the other hand, DPPT-TT and P-18 showed slight or negligible red shift with the same λ_{max} between the solution and film. These spectral characteristics in DPPT-TT and P-18 can be associated with the formation of aggregates in the solutions prior to deposition through strong interchain interaction of those polymers and limited solubility. Indeed, DPP moieties are already known to possess remarkable aggregating properties, and pre-aggregation of P-18 polymer has been previously proved by measuring the temperature dependence of absorption in the solution.[36-38] To check solvent dependency for the formation of pre-aggregation, P(NDI2OD-T2) was dissolved in chlorobenzene (CB) and toluene (Tol). The absorption spectra of both solutions were recorded, along with the spectra of the spin-coated films. Although both spectra for P(NDI2OD-T2) films are similar, the spectra measured for the solution in CB is more red-shifted than that for the Tol solution. Such pre-aggregation in P(NDI2OD-T2) solution has previously been reported to affect the size of fibrils at the film surface, which develop anisotropically and form domains with a marked orientational alignment.[27,39,40] The alignment present at the semiconductor film surfaces were observed by atomic force microscopy (AFM) via grain analysis mode (Figure S1), and the surface morphologies are strongly consistent with the UV-vis-NIR absorption spectra. The films deposited from solutions with well-dispersed polymers, such as P3HT, showed smoother surface with smaller size of domains than films from pre-aggregated solutions, such as DPPT-TT, P-18, and P(NDI2OD-T2). The films for DPPT-TT, P-18, and P(NDI2OD-T2) from Tol showed much wider domain size than the P3HT and P(NDI2OD-T2) films from the CB solution. The schematic illustration in Figure 2f suggests the formation of aligned polymer films when a high degree of pre-aggregation is present in the solution, and the deposition is performed by off-center spin-coating.

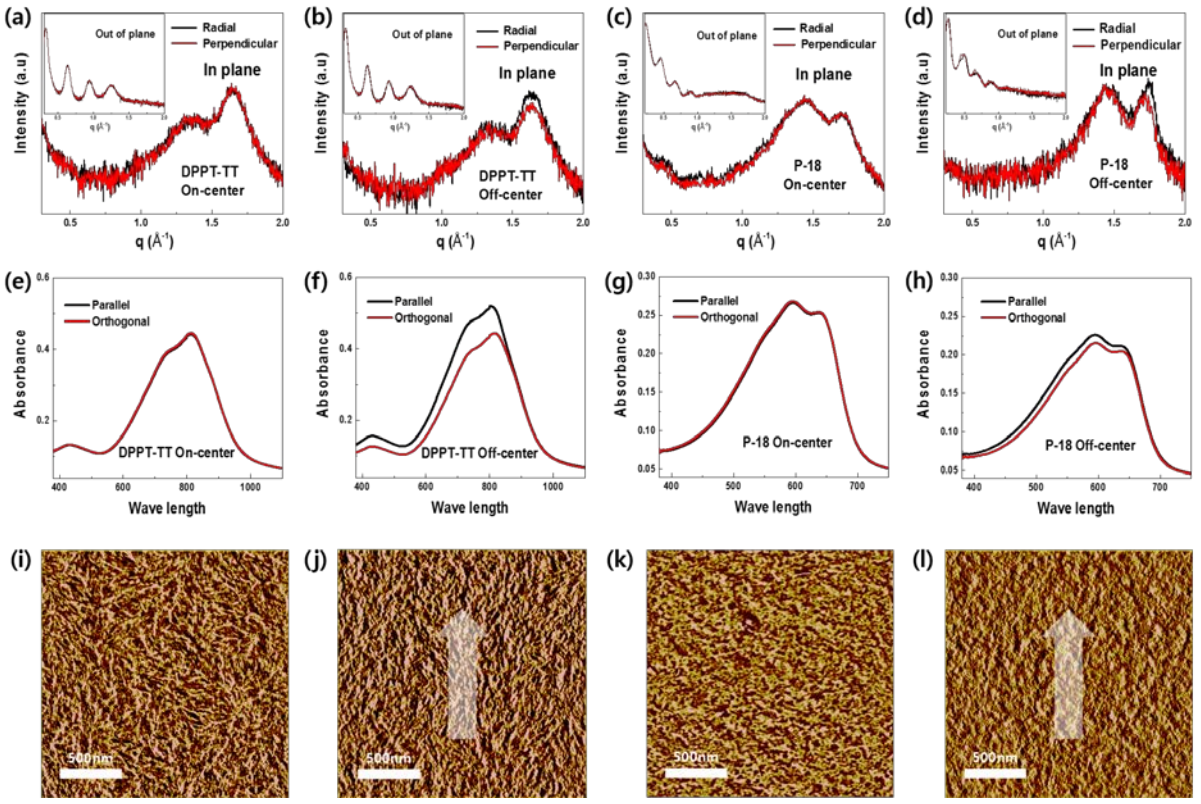

Figure 3. GIXD for on-center spin-coated (a) DPPT-TT and (c) P-18, and off-center spin-coated (b) DPPT-TT and (d) P-18 films. UV-vis-NIR absorption spectra for on-center spin-coated (e) DPPT-TT and (g) P-18, and off-center spin-coated (f) DPPT-TT and (h) P-18 films. Tapping mode AFM phase images for (i) DPPT-TT and (k) P-18 by on-center spin-coating method, and off-center coated (j) DPPT-TT and (l) P-18. Arrow in (j) and (l) indicates coating direction.

To confirm the presence of an anisotropic polymer chain alignment in the bulk of DPPT-TT and P-18 films, we measured GIXD and polarized UV-vis-NIR absorption (Figure 3a- 3h). In order to demonstrate the polymer chain alignment, we compared the data obtained by employing the off-center spin-coating method with the data obtained with conventionally on-center spin-coated films. Every sample was measured at the center of the film by recording two different measurements, one with a 90° rotation with respect to the radial direction parallel, and orthogonal to the polarized UV-vis-NIR and X-ray direction.

In the GIXD data, all measured DPPT-TT and P-18 films showed the intense out-of-plane diffraction peaks of q_z at approximately 0.32 $Å^{-1}$ and 0.25 $Å^{-1}$ that indicate strong edge-on

orientation of polymer molecules with lamella *d*-spacing of 19.64 Å and 25.13 Å, respectively (Figure 3a-3d). In addition, in-plane diffraction peaks of q_{xy} at approximately 1.63 $Å^{-1}$ and 1.72 $Å^{-1}$ that correspond to the π-π distance of 3.86 Å and 3.65 Å were observed in the DPPT-TT and P-18 films, respectively. The on-center spin-coated films of DPPT-TT and P-18 showed exactly the same intensity regardless of the sample orientation (in-plane and out-of-plane, Figure 3a and 3c). The off-center spin-coated films showed an very little intensity difference only in the in-plane peaks, but no difference in the out-of-plane peaks (Figure 3b and 3d). These results indicate that off-center spin-coated films show only a small structural anisotropy in the bulk of films, even if strong centrifugal and centripetal forces are applied during the coating process. Similar information is provided by the polarized UV-vis-NIR spectra of DPPT-TT and P-18 off-center films, where there is a strong dependence on the relative peak intensity according to the parallel and orthogonal sample orientation (Figure 3f, 3h). The samples prepared with the on-centered method instead did not show any dependence on beam polarization. The optical dichroic ratio, given by the ratio between peak intensity for the parallel and orthogonal orientations, is found to be 1 (at λ = 550 nm) for the unaligned films (P3HT and on-center coated DPPT-TT and P-18 films), and 1.17 (at λ = 820 nm), 1.07 (at λ = 600 nm), 1.04 (at λ = 705 nm), and 1.04 (at λ = 705 nm) for the off-center coated DPPT-TT, P-18, P(NDI2OD-T2) spun from CB, and P(NDI2OD-T2) spun from Tol, respectively (Table 1). Therefore, the absorption and GIXD spectra reveal the presence of only a small optical and structural anisotropy in the films, although these samples were prepared with the off-center spin-coating method. Since both techniques mostly deliver information about the bulk of the films, we further investigated the presence of a possible stronger anisotropy at the film surfaces.

First, we acquired surface topography AFM images (Figure 3i-l). The phase images of on-center spin-coated films reveal randomly-aligned domain formations (Figure 3i, 3k), whereas off-center spin-coated films show the formation of domains with good alignment in the

direction of the arrow that corresponds with the radial coating direction (Figure 3j, 3l).

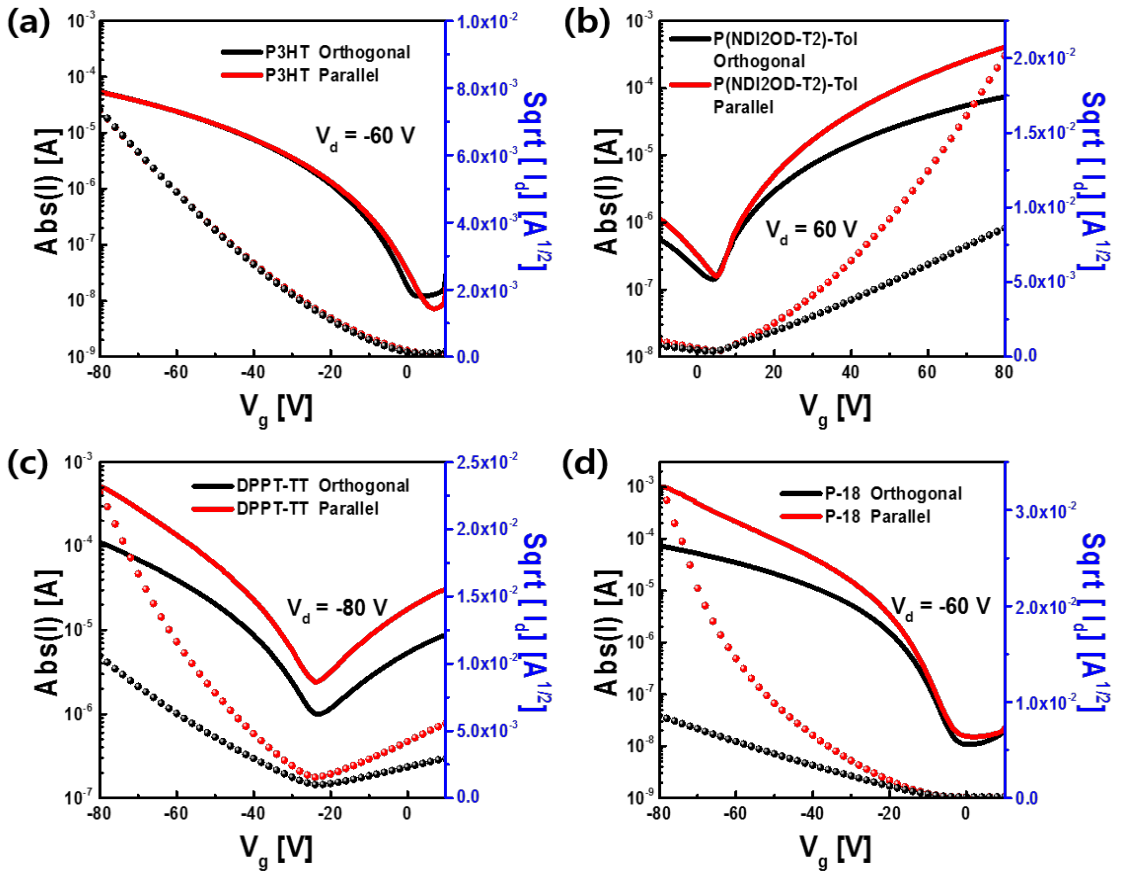

Figure 4. Transfer characteristics of anisotropic (a) P3HT, (b) P(NDI2OD-T2) in Tol, (c) DPPT-TT, and (d) P-18 OTFTs (W/L = 1.0 mm/20 μm).

We also fabricated top gate/bottom contact OFETs by off-center spin-coating in order to probe the transport properties in the first molecular layers from the interface with the dielectric, and we compared the effect of chain alignment that was orthogonal or parallel with respect to the channel. We measured μ_{FET} of an off-center spin-coated DPPT-TT based OFET by placing the electrode pattern at different distances from the spinning center (Figure S2). The anisotropy of μ_{FET} increased gradually with distance, and it is saturated at 2 cm, which is considered the optimal relative distance for the following data: Figure 4a-d show representative transfer curves for the off-center spin-coated P3HT, P(NDI2OD-T2), DPPT-TT, and P-18 OFETs with channel direction parallel and orthogonal to the spinning direction (see Figure 1b). All basic device parameters are summarized in Table 1. The P3HT device showed almost the same

transfer curves and μ_{FET} regardless of the coating direction. In contrast, a significantly large anisotropy of electrical properties was observed in DPPT-TT and P-18 OFETs, with a 6 and 37-fold improvement in μ_{FET}, respectively. Compared with conventional on-center spin-coated devices, μ_h for DPPT-TT and P-18 OFETs showed a significant increase in the parallel aligned sample going from 0.66 (±0.20) cm^2/Vs and 2.06 (±2.15) cm^2/Vs, to 2.05 (±0.30) cm^2/Vs (maximum mobility, μ_{max} = 2.48 cm^2/Vs) and 5.66 (±1.71) cm^2/Vs (μ_{max} = 7.25 cm^2/Vs), respectively. Interestingly, the devices with off-center spin-coated DPPT-TT film without post-thermal annealing process showed equivalent or even higher performance compared with the thermal annealed on-center spin-coated one (Table 1). In addition, the devices coated in the parallel direction showed not only higher μ_{FET}, but also lower relative standard deviation of μ_{FET} compared with on-center spin-coated devices, from 30% to 15% and from 104% to 30% by uniform polymer alignment in DPPT-TT and P-18 OFETs, respectively.

We also investigated the effect of pre-aggregating P(NDI2OD-T2) to different solvents on the favorable alignment induced by off-center spin-coating. We already observed the strong dependence of the electron mobility on the parallel or orthogonal orientation when spun from CB ($\mu_{//} / \mu_{\perp}$ = 5). This ratio strongly increases ($\mu_{//} / \mu_{\perp}$ = 9) when Tol is used as a solvent.

We then performed *polarized*-charge modulation microscopy (p-CMM) on operating field-effect transistors. *p*-CMM is a micro-spectroscopy technique that can be adopted to detect and quantify domains within the accumulated channels of OFETs characterized by orientational alignment of charge-induced transition dipole moments; a direct correlation with the surface film micro-structure is also possible if the relative orientation of the charge transition dipole moment and polymer chain is known.[41] In CMM, the probed signal is represented by the spectral features induced by localized charge carriers, i.e. the variation of the transmission, normalized to the total transmission, induced by the presence of relaxed charge species in the polymer semiconductor. Therefore, this technique is inherently sensitive to the accumulated

channel volume at the interface between the semiconductor and dielectric, and more specifically, to the sole conjugated segments probed by charge carriers.[35]

We acquired the charge modulation spectra (CMS) locally within the channel for each polymer (Figure S3). The spectra are reproducible over different sampling areas and are consistent with the reported film absorption spectra. We then performed charge modulation mapping by probing the DPPT-TT sample at 820 nm and the P-18 sample at 600 nm, i.e., in correspondence to the bleaching signal of the main absorption peak. In Figure 5, we show the transition dipole moment (TDM) orientation maps and the maps of degree of order (DO).[41] The degree of order represents the ratio of the aligned transition dipole moments with respect to the total amount of the charge-modulated signal.

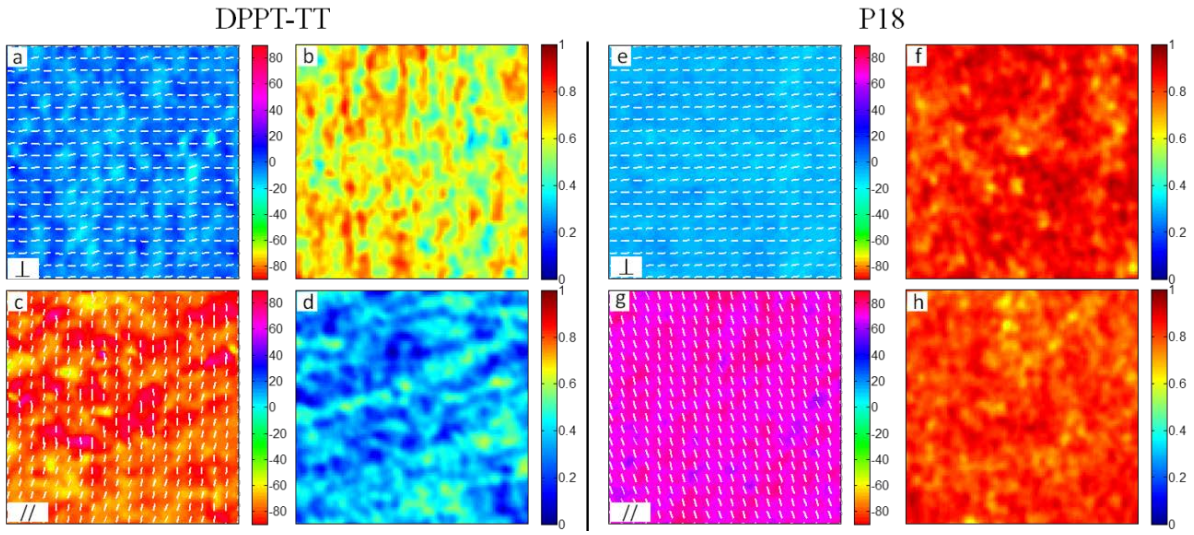

Figure 5. *p*-CMM data analysis for DPPT-TT and P-18 devices. Mapping areas are 35 × 35 μm^2. Local orientation for aligned fraction of polymeric backbones as calculated from CMS data of a device with semiconducting DPPT-TT: (a) orthogonal, (c) parallel and P-18, (e) orthogonal, (g) parallel. Local degree of alignment relative to map of panel with DPPT-TT: (b) orthogonal, (d) parallel and P-18, (f) orthogonal, (h) parallel. In all maps, electrodes can be found at plot's left and right sides.

For both orthogonal samples of DPPT-TT and P-18, the angular maps show that a high density of dipole moments of the ground state transition at 820 nm and 600 nm, respectively, aligned orthogonally to the channel, is present (Figure 5a, 5b, 5e, and 5f). The maps recorded

on the parallel samples correspondingly indicate a preferential orientation along the direction parallel to the channel. This is consistent with the expected chain orientation due to the spin conditions, suggesting that the conjugated chain and transition dipole moment of the ground state absorption are aligned along the same direction. All maps also show good DO in the channel. In the case of P-18, the average DO values are 84% and 81% for the orthogonal and parallel samples, respectively. DO for DPPT-TT is still relatively good, but it is lower than that for P-18, with average values of 60% and 35% for the orthogonal and parallel samples, respectively. We have to indicate that the degree of order provides information on the polymer anisotropy across the channel, but it is a correct estimation of the chain alignment along the conduction channel only if the polymer chains lay parallel to the substrate. It is possible to evaluate the dichroic ratio from the *p*-CMM measurements according to

$$Dichroic\ \ ratio = \frac{1+\mathrm{DO\ \ parallel}}{1-\mathrm{DO\ \ orthogonal}} \quad (1)$$

The calculated ratios are 3.4 and 11.3 in the DPPT-TT and P-18 films, respectively, and these are better matched with the anisotropy of the electronic properties in OFETs. These values are remarkably enhanced with respect to the optical dichroic ratio based on UV-vis-NIR absorption spectra and in-plane intensity difference in GXID, implying that anisotropy in the conjugated segments probed by charges in the few-nanometers-thick channel at the interface with the dielectric is much stronger than the average alignment of all molecules in the bulk of the film.

AFM, TG/BC OFETs performance and *p*-CMM data confirm that a strong alignment of the polymer chains is occurring at the top interface between the semiconductors and dielectrics. In order to address the eventual alignment possibly occurring also at the bottom surface, we compared the μ_{FET} of a dual gate OFET. The device structure consists of a film of off-centered

spin-coated DPPT-TT, a PMMA layer as the top dielectric contact, and SiO_2 as the bottom dielectric (Figure S4). For the bottom gate/bottom contact (BG/BC) geometry, we found μ_{FET} of 0.011 cm^2/Vs for both the orthogonal and parallel orientations. For the top gate devices, we instead found large μ_{FET} anisotropy with 0.6 cm^2/Vs and 0.2 cm^2/Vs for the parallel and orthogonal orientations, respectively. The BG/BC devices showed relatively lower performance because of higher contact resistance (R_c), and likely because of the presence of charge trap states at the SiO_2 dielectric and DPPT-TT interface. Given that the transistor channel is known to form within a few molecular layers close to the dielectric interface,[42] these results confirm that a much higher anisotropy in the polymer chain alignment is present at the top polymer interface with respect to the bottom interface.

The reason for such different anisotropy at the top and bottom interfaces can be ascribed to the different surface energies experienced by the polymer interfaces. The bottom interface is characterized by a high surface energy induced by oxygen UV/O_3 treatment,[43] whereas subsequent molecular layers experience much weaker adhesive forces because of the lower surface energy induced by the first deposited layers, likely favoring a more effective alignment.

We measured R_c for on-center and off-center-coated DPPT-TT-based OFETs by the transfer-line method (TLM) (Figure S5). The width-normalized contact resistance R_cW of both DPPT-TT OFETs is very similar for on-center, off-center parallel, and orthogonal samples. Therefore, the significant enhancement of μ_h is mainly caused by a more efficient charge in the surface aligned polymer chains and cannot be explained instead with a modification of the charge injection properties. We also measured the mobility activation energy (E_A) by the variable temperature measurements of DPPT-TT OFETs prepared with different coating directions (Figure S6). Very interestingly, on-center, orthogonal, and parallel-coated devices showed very similar E_A of 40.4 meV, 39.3 meV, and 51.5 meV, respectively, as extracted in the temperature range from 297 K to 140 K. These results are consistent with previous reports

on OFETs by aligned polymer film.[21,44] The typical length of a straight chain segment is much shorter than the channel length of an OFET, and many inter-chain hopping events are necessary for the charge carrier to be transported from source to drain. Within this framework, similar activation energies for different mobilities for each coating direction indicate that the inter-chain hopping rate is independent with respect to the direction of the electric field, whereas mobility anisotropy arises by a modulation of the average drift distance for a charge carrier between two hopping steps.

Table 1. OFETs performances and dichroic ratio of various semiconductor materials with different conditions.

Semiconductor	**Coating Direction /Annealing**	**Mobility (cm^2/Vs)**	**Standard Deviation**	**Dichroic Ratio (UV-vis-NIR)**	**Dichroic Ratio (*p*-CMM)**
DPPT-TT	On-center/200°C	0.66(±0.20)	30%	1	
	Parallel/RT	0.70(±0.12)	17%		
	Orthogonal/200°C	0.35(±0.05)	14%	1.17	3.38
	Parallel/200°C	2.05(±0.30)	15%		
P-18	On-center/250°C	2.06(±2.15)	104%	1	
	Orthogonal/250°C	0.15(±0.03)	20%	1.07	11.31
	Parallel/250°C	5.66(±1.71)	30%		
P3HT	Orthogonal/150°C	0.087(±0.004)	5%	1	
	Parallel/150°C	0.088(±0.010)	11%		
P(NDI2OD-T2)-CB	Orthogonal/200°C	0.12(±0.02)	17%	1.04	

	Parallel/200°C	0.60(±0.07)	12%	
P(NDI2OD-T2)-Tol	Orthogonal/200°C	0.11(±0.03)	27%	1.04
	Parallel/200°C	0.95(±0.09)	10%	

*The mobility (μ_{FETs}) was calculated at the saturation region (gate voltage in the last 10V of transfer curves (from -70 to -80V)) for 5 to 10 devices, [DPPT-TT: at V_d = -80V; P-18: at V_d = -60V; P3HT: at V_d = -60V; P(NDI2OD-T2): at V_d = 60V] using gradual channel approximation equations. (W/L = 1.0 mm/20μm, whereas PMMA gate dielectric thickness and capacitance were ~500 nm and ~6.2 nF/cm^2, respectively.)

CONCLUSION

In conclusion, we demonstrated higher performance reached by OFETs, where the semiconducting polymer is aligned by off-center spin-coating. The formation of an anisotropic thin film is shown to be strongly correlated with the degree of pre-aggregation in the solution for a wide range of donor-acceptor copolymers. The strong alignment of the polymer chains was found to be dominant only at the polymer surface in the off-center spin-coating process, a sufficient condition for largely improving hopping transport and narrowing data dispersion in field-effect devices. This study indicates that controlling the orientation and alignment of polymer chains has the potential for delivering excellent electrical properties with good reliability in OFETs.

EXPERIMENTAL METHODS

Field-Effect Transistor Fabrication. Pre-patterned Corning Eagle 2000 glass substrates were cleaned sequentially in an ultrasonic bath with de-ionized water, acetone, and iso-propanol for 15 min per solvent. The Au/Ni (15 nm/5 nm thick) patterns used as source and drain electrodes were fabricated using conventional photolithography. Before coating with

semiconducting polymer solutions, the substrates were treated by oxygen UV/O_3 for 20 min. The semiconductor material, P-18, was synthesized in our laboratory using a previously published procedure,[36] and it was dissolved in anhydrous dichlorobenzene (DCB) to obtain a solution with the concentration of 7 mg/ml. DPPT-TT, P3HT (purchased from Sigma Aldrich), and P(NDI2OD-T2) (purchased from Polyera Corporation) solutions were prepared with a concentration of 10 mg/ml in chlorobenzene (CB) or 5 mg/ml in toluene (Tol). These were off-center spin-coated at 1,500 rpm (3-second acceleration) in an N_2-purged glove box, where the electrode pattern was placed 20 mm away from the rotation axis of the spin-coater. All semiconductor layer thickness were 30~50 nm and those were measured by a surface profiler (Kosaka ET-3000i).

The DPPT-TT and P(NDI2OD-T2) films were thermally annealed at 200 °C, and the P3HT and P-18 films were annealed at 150 °C and 250 °C for 20 min, respectively, to remove the residual solvents and induce an ordered crystalline phase in a glove box with N_2 atmosphere. PMMA (Aldrich, M_w = 120 kD) was used as dielectric material without further purification. PMMA (80 mg/ml) was dissolved in n-butylacetate, and the solution was filtered with a 0.45 μm PTFE syringe filter before spin-coating. After deposition, the devices were baked at 80 °C for 2 hours under N_2 conditions. Transistor fabrication was completed by deposition of aluminum top-gate electrode by thermal evaporation (~50 nm thick) using metal shadow masks.

Thin Film and Device Characterizations. The surface morphologies of semiconducting polymer films were investigated by tapping-mode AFM (Nanoscope III, Veeco Instruments, Inc.). UV–vis spectrometry was conducted using a Perkin Elmer Lambda 750, and a polarized film was used in front of the beam source. The OFET electrical characteristics were measured using a semiconductor parameter analyzer (Keithley 4200-SCS) in an N_2-filled glove box. The field-effect mobility (μ_{FET}) was calculated from the saturation regime using equations for

classical silicon MOSFETs.

Polarized Charge Modulation Microscopy. The *p*-CMM data were collected with a homemade confocal microscope that operated in transmission mode.

The light source consisted of a supercontinuum laser (NKT Photonics, SuperK Extreme) monochromated by an acousto-optic modulator (NKT Photonics, SuperK Select) in the 500-1000 nm region with line widths between 2 nm and 5 nm. Laser polarization was controlled with a half-wave plate and linear polarizer. The light was then focused on the sample with 0.7 N.A. objective (S Plan Fluor60_, Nikon) and collected by a second 0.75 N.A. objective (CFI Plan Apochromat VC 20_, Nikon). The collected light was focused on the entrance of a multimodal glass fiber with 50 μm core that acted as confocal aperture. Detection was operated through a silicon photodetector (FDS100, Thorlabs). The signal was amplified by a transimpedance amplifier (DHPCA-100, Femto) and supplied both to DAQ (to record the transmission signal, T) and a lock-in amplifier (SR830 DSP, Stanford Research Systems) in order to retrieve the differential transmission data, ΔT. The system was run with custom LabVIEW software. The OD values were obtained from T as described in the Supplementary Discussion, whereas the CMS data were calculated as ΔT/T. The sample was stored in an inert atmosphere by fluxing nitrogen in a homemade chamber. The gate voltage of the transistor was sinusoidally modulated at 989 Hz between 20 V and 60 V with a waveform generator (3390, Keithley) amplified by a high-voltage amplifier (WMA-300, Falco Systems), whereas the source and drain contacts were maintained at short-circuit. Signal maps were collected by raster-scanning the sample at 250 ms per pixel with a lock-in integration time of 100 ms. All data were processed with MATLAB software. OD and CMS images were smoothed by convolution with a bell-shaped function.

ASSOCIATED CONTENT

Supporting Information (SI) atomic force microscopy images, anisotropic dependence of charge transport properties, charge modulation spectra analysis, transfer and output characteristics, contact resistance, temperature-dependent mobility of DPPT-TT OFETs. This information is available free of charge via the internet at http://pubs.acs.org/.

Author Information

Corresponding Author

*E-mail: yynoh@dongguk.edu (Y.-Y. Noh), kimdy@gist.ac.kr (D.-Y. Kim).

ACKNOWLEDGMENT

This work was supported by the Center for Advanced Soft-Electronics (2013M3A6A5073183) funded by the Korean Government (MSIP), "Basic Research Projects in High-tech Industrial Technology" Project through a grant provided by GIST in 2015, the Pioneer Research Center Program through the National Research Foundation of Korea funded by the Ministry of Science, ICT & Future Planning (NRF-2013M3C1A3065528), and the National Research Foundation of Korea (NRF) grant funded by the MSIP (NRF-2014R1A2A2A01007159). M. C. acknowledges financial support by the European Research Council (ERC) under the European Union's Horizon 2020 research and innovation program "HEROIC", grant agreement 638059. The GIXD was measured using the synchrotron radiation sources 9C beam line at the Pohang Accelerator Laboratory (PAL). We thank the Korea Basic Science Institute (KBSI) for AFM measurement facilities.

Reference

(1) Forrest, S. R. The Path to Ubiquitous and Low-cost Organic Electronic Appliances on Plastic. *Nature,* **2004**, *428*, 911-918.
(2) Sirringhaus, H. Organic Field-Effect Transistors: The Path Beyond Amorphous Silicon. *Adv. Mater*., **2014**, *26*, 1319-1335.
(3) Baeg, K. J.; Caironi, M.; Noh, Y. Y. Toward Printed Integrated Circuits based on Unipolar or Ambipolar Polymer Semiconductors. *Adv. Mater*., **2013**, *25*, 4210-4244.
(4) Minemawari, H.; Yamada, T.; Matsui, H.; Tsutsumi, J.; Haas, S.; Chiba, R.; Kumai, R.; Hasegawa, T. Inkjet Printing of Single-crystal Films. *Nature*, **2011**, *475*, 364-367.
(5) Diao, Y.; Tee, B. C.; Giri, G.; Xu, J.; Kim, D. H.; Becerril, H. A.; Stoltenberg, R. M.; Lee, T. H.; Xue, G.; Mannsfeld, S. C. Solution Coating of Large-area Organic Semiconductor Thin Films with Aligned Single-crystalline Domains. *Nat. Mater*., **2013**, *12*, 665-671.
(6) Tseng, H. R.; Phan, H.; Luo, C.; Wang, M.; Perez, L. A.; Patel, S. N.; Ying, L.; Kramer, E. J.; Nguyen, T. Q.; Bazan, G. C.; Heeger, A. J. High-Mobility Field-Effect Transistors Fabricated with Macroscopic Aligned Semiconducting Polymers. *Adv. Mater*., **2014**, *26*, 2993-2998.
(7) Yuan, Y.; Giri, G.; Ayzner, A. L.; Zoombelt, A. P.; Mannsfeld, S. C.; Chen, J.; Nordlund, D.; Toney, M. F.; Huang, J.; Bao, Z. Ultra-high Mobility Transparent Organic Thin Film Transistors Grown by an Off-centre Spin-coating Method. *Nat. Commun.*, **2014**, *5*, 3005.
(8) Nakayama, K.; Hirose, Y.; Soeda, J.; Yoshizumi, M.; Uemura, T.; Uno, M.; Li, W.; Kang, M. J.; Yamagishi, M.; Okada, Y. Patternable Solution-Crystallized Organic Transistors with High Charge Carrier Mobility. *Adv. Mater*., **2011**, *23*, 1626-1629.
(9) Facchetti, A. π-Conjugated Polymers for Organic Electronics and Photovoltaic Cell Applications. *Chem. Mater*., **2011**, *23*, 733-758.
(10) Matsidik, R.; Komber, H.; Luzio, A.; Caironi, M.; Sommer, M. Defect-free Naphthalene Diimide Bithiophene Copolymers with Controlled Molar Mass and High Performance via Direct Arylation Polycondensation *J. Am. Chem. Soc*., **2015**, 137, 6705-6711.
(11) Nicolai, H.; Kuik, M.; Wetzelaer, G.; De Boer, B.; Campbell, C.; Risko, C.; Brédas, J.; Blom, P. Unification of Trap-limited Electron Transport in Semiconducting Polymers. *Nat. Mater*., **2012**, *11*, 882-887.
(12) Nugraha, M. I.; Häusermann, R.; Bisri, S. Z.; Matsui, H.; Sytnyk, M.; Heiss, W.; Takeya, J.; Loi, M. A. High Mobility and Low Density of Trap States in DualSolid-Gated PbS Nanocrystal Field-Effect Transistors. *Adv. Mater*., **2015**, *27*, 2107-2112.
(13)Yan, H.; Chen, Z.; Zheng, Y.; Newman, C.; Quinn, J. R.; Dötz, F.; Kastler, M.; Facchetti, A. A high-mobility electron-transporting polymer for printed transistors. *Nature*, **2009,** *457*, 679-686.
(14) Kim, B.-G.; Jeong, E. J.; Chung, J. W.; Seo, S.; Koo, B.; Kim, J. A Molecular Design Principle of Lyotropic Liquidcrystalline Conjugated Polymers with Directed Alignment Capability for Plastic Electronics. *Nat. Mater*., **2013**, *12*, 659-664.
(15) Nketia-Yawson, B.; Lee, H. S.; Seo, D.; Yoon, Y.; Park, W. T.; Kwak, K.; Son, H. J.; Kim, B.; Noh, Y. Y. A Highly Planar Fluorinated Benzothiadiazole-Based Conjugated Polymer for High-Performance Organic Thin-Film Transistors. *Adv. Mater*., **2015**, *27*, 3045-3052.
(16) Tsao, H. N.; Cho, D. M.; Park, I.; Hansen, M. R.; Mavrinskiy, A.; Yoon do, Y.; Graf, R.; Pisula, W.; Spiess, H. W.; Mullen, K. Ultrahigh Mobility in Polymer Field-Effect Transistors

by Design. *J. Am. Chem. Soc.*, **2011**, *133*, 2605-2612.
(17) Chen, Z.; Lee, M. J.; Shahid Ashraf, R.; Gu, Y.; Albert-Seifried, S.; Meedom Nielsen, M.; Schroeder, B.; Anthopoulos, T. D.; Heeney, M.; McCulloch, I.; Sirringhaus, H. High-Performance Ambipolar Diketopyrrolopyrrole-Thieno[3,2-*b*]thiophene Copolymer Field-Effect Transistors with Balanced Hole and Electron Mobilities. *Adv. Mater.*, **2012**, *24*, 647-652.
(18) Khim, D.; Baeg, K. J.; Kim, J.; Kang, M.; Lee, S. H.; Chen, Z.; Facchetti, A.; Kim, D. Y.; Noh, Y. Y. High Performance and Stable N-Channel Organic Field-Effect Transistors by Patterned Solvent-Vapor Annealing. *ACS Appl. Mater. Interfaces*, **2013**, *5*, 10745-10752.
(19) Kim, N.-K.; Khim, D.; Xu, Y.; Lee, S.-H.; Kang, M.; Kim, J.; Facchetti, A.; Noh, Y.-Y.; Kim, D.-Y. Solution-Processed Barium Salts as Charge Injection Layers for High Performance N-Channel Organic Field-Effect Transistors. *ACS Appl. Mater. Interfaces*, **2014**, *6*, 9614-9621.
(20) Kim, J.; Khim, D.; Kang, R.; Lee, S.-H.; Baeg, K.-J.; Kang, M.; Noh, Y.-Y.; Kim, D.-Y. Simultaneous Enhancement of Electron Injection and Air Stability in N-Type Organic Field-Effect Transistors by Water-Soluble Polyfluorene Interlayers. *ACS Appl. Mater. Interfaces*, **2014**, *6*, 8108-8114.
(21) Sirringhaus, H.; Wilson, R. J.; Friend, R. H.; Inbasekaran, M.; Wu, W.; Woo, E. P.; Grell, M.; Bradley, D. D. C. Mobility Enhancement in Conjugated Polymer Field-effect Transistors through Chain Alignment in a Liquid-crystalline Phase. *Appl. Phys. Lett.*, **2000**, *77*, 406-408.
(22) Sakamoto, K.; Yasuda, T.; Miki, K.; Chikamatsu, M.; Azumi, R. Anisotropic Field-effect Hole Mobility of Liquid Crystalline Conjugated Polymer Layers Formed on Photoaligned Polyimide Films. *J. Appl. Phys.*, **2011**, *109*, 013702.
(23) Tseng, H. R.; Ying, L.; Hsu, B. B.; Perez, L. A.; Takacs, C. J.; Bazan, G. C.; Heeger, A. J. High Mobility Field Effect Transistors Based on Macroscopically Oriented Regioregular Copolymers. *Nano Lett.*, **2012**, *12*, 6353-6357.
(24) Shin, J.; Hong, T. R.; Lee, T. W.; Kim, A.; Kim, Y. H.; Cho, M. J.; Choi, D. H. Template-Guided Solution-Shearing Method for Enhanced Charge Carrier Mobility in Diketopyrrolopyrrole-Based Polymer Field-Effect Transistors. *Adv. Mater.*, **2014**, *26*, 6031-6035.
(25) Becerril, H. A.; Roberts, M. E.; Liu, Z.; Locklin, J.; Bao, Z. High-Performance Organic Thin-Film Transistors through Solution-Sheared Deposition of Small-Molecule Organic Semiconductors. *Adv. Mater.*, **2008**, *20*, 2588-2594.
(26) Wang, H.; Chen, L.; Xing, R.; Liu, J.; Han, Y. Simultaneous Control over both Molecular Order and Long-Range Alignment in Films of the Donor−Acceptor Copolymer. *Langmuir*, **2015**, *31*, 469-479.
(27) Luzio, A.; Criante, L.; D'Innocenzo, V.; Caironi, M. Control of Charge Transport in a Semiconducting Copolymer by Solvent-induced Long-range Order. *Sci. Rep.*, **2013**, *3*, 3425.
(28) Yang, H.; Shin, T. J.; Yang, L.; Cho, K.; Ryu, C. Y.; Bao, Z. Effect of Mesoscale Crystalline Structure on the Filed-Effct Mobility of Regioregular Poly(3-hexyl thiophene) in Thin-film Transistor. *Adv. Funct. Mater.*, **2005**, *15*, 671-676.
(29) Park, Y. D.; Lee, H. S.; Choi, Y. J.; Kwak, D.; Cho, J. H.; Lee, S.; Cho, K. Solubility-Induced Ordered Polythiophene Precursors for High-Performance Organic Thin-Film Transistors. *Adv. Funct. Mater.*, **2009**, *19*, 1200-1206.
(30) Bucella, S. G.; Luzio, A.; Gann, E.; Thomsen, L. McNeill, C. R.; Pace, G.; Perinot, A.; Chen, Z.; Facchetti, A.; Caironi, M. Macroscopic and high-throughput printing of aligned nanostructured polymer semiconductors for MHz large-area electronics. *Nat. Commun.*, **2015**, *6*, 8394.
(31) Duong, D. T.; Ho, V.; Shang, Z.; Mollinger, S.; Mannsfeld, S. C. B.; Dacuña, J.; Toney,

M. F.; Segalman, R.; Salleo, A. Mechanism of Crystallization and Implications for Charge Transport in Poly(3-ethylhexylthiophene) Thin Films. *Adv. Funct. Mater.*, **2014**, *24*, 4515-4521.
(32) Chen, H.; Guo, Y.; Yu, G.; Zhao, Y.; Zhang, J.; Gao, D.; Liu, H.; Liu, Y. Highly π - Extended Copolymers with Diketopyrrolopyrrole Moieties for High-Performance Field-Effect Transistors. *Adv. Mater.*, **2012**, *24*, 4618-4622.
(33) Lee, J.; Han, A. R.; Yu, H.; Shin, T. J.; Yang, C.; Oh, J. H. Boosting the Ambipolar Performance of Solution-Processable Polymer Semiconductors via Hybrid Side-Chain Engineering. *J. Am. Chem. Soc.*, **2013**, *135*, 9540-9547.
(34) Bronstein, H.; Chen, Z.; Ashraf, R. S.; Zhang, W.; Du, J.; Durrant, J. R.; Tuladhar, P. S.; Song, K.; Watkins, S. E.; Geerts, Y.; Wienk, M. M.; Janssen, R. A.; Anthopoulos, T.; Sirringhaus, H.; Heeney, M.; McCulloch, I. Thieno[3,2-b]thiophene-Diketopyrrolopyrrole-Containing Polymers for High-Performance Organic Field-Effect Transistors and Organic Photovoltaic Devices. *J. Am. Chem. Soc.*, **2011**, *133*, 3272-3275.
(35) Sciascia, C.; Martino, N.; Schuettfort, T.; Watts, B.; Grancini, G.; Antognazza, M. R.; Zavelani-Rossi, M.; McNeill, C. R.; Caironi, M. Sub-Micrometer Charge Modulation Microscopy of a High Mobility Polymeric n-Channel Field-Effect Transistor. *Adv. Mater.*, **2011**, *23*, 5086-5090.
(36) Jang, S.-Y.; Kim, I.-B.; Kim, J.; Khim, D.; Jung, E.; Kang, B.; Lim, B.; Kim, Y.-A.; Jang, Y. H.; Cho, K.; Kim, D.-Y. New Donor−Donor Type Copolymers with Rigid and Coplanar Structures for High-Mobility Organic Field-Effect Transistors. *Chem. Mater.*, **2014**, *26*, 6907-6910.
(37) Nielsen, C. B.; Turbiez, M.; McCulloch, I. Recent Advances in the Development of Semiconducting DPP-Containing Polymers for Transistor Applications. *Adv. Mater.*, **2013**, *25*, 1859-1880.
(38) Li, Y.; Sonar, P.; Murphy, L.; Hong, W. High Mobility Diketopyrrolopyrrole (DPP)-Based Organic Semiconductor Materials for Organic Thin Film Transistors and Photovoltaics. *Energy Environ. Sci.* **2013**, *6*, 1684-1710.
(39) Steyrleuthner, R.; Schubert, M.; Howard, I.; Klaumunzer, B.; Schilling, K.; Chen, Z.; Saalfrank, P.; Laquai, F.; Facchetti, A.; Neher, D. Aggregation in a High-Mobility n-Type Low-Bandgap Copolymer with Implications on Semicrystalline Morphology. *J. Am. Chem. Soc.*, **2012**, *134*, 18303-18317.
(40) Steyrleuthner, R.; Di Pietro, R.; Collins, B. A.; Polzer, F.; Himmelberger, S.; Schubert, M.; Chen, Z.; Zhang, S.; Salleo, A.; Ade, H.; Facchetti, A.; Neher, D. The Role of Regioregularity, Crystallinity, and Chain Orientation on Electron Transport in a High-Mobility n-Type Copolymer. *J. Am. Chem. Soc.*, **2014**, *136*, 4245-4256.
(41) Martino, N.; Fazzi, D.; Sciascia, C.; Luzio, A.; Antognazza, M. R.; Caironi, M. Mapping Orientational Order of Charge-Probed Domains in a Semiconducting Polymer. *ACS nano*, **2014**, *8*, 5968-5978.
(42) Zaumseil, J.; Sirringhaus, H. Electron and Ambipolar Transport in Organic Field-Effect Transistors. *Chem. Rev.*, **2007**, *107*, 1296-1323.
(43) Yang, S. Y.; Shin, K.; Park, C. E. The Effect of Gate-Dielectric Surface Energy on Pentancene Morphology and Organic Field-Effect Transistor Characteristics. *Adv. Funct. Mater.*, **2005**, *15*, 1806-1814.
(44) Bussac, M.; Zuppiroli, L. High-Field Mobility in an Assembly of Conjugated Polymer Segments. *Phys. Rev. B*, **1996**, *54*, 4674-4679.